



Characterizing spontaneous irregular behavior in coupled map lattices

York Dobyns^a, Harald Atmanspacher^{b,*}

^a *PEAR, Princeton University Princeton, NJ 08544-5263, USA*

^b *Institut für Grenzgebiete der Psychologie und Psychohygiene Wilhelmstrasse 3a, Freiburg 79098, Germany*

Accepted 14 September 2004

Abstract

Two-dimensional coupled map lattices display, in a specific parameter range, a stable phase (quasi-) periodic in both space and time. With small changes to the model parameters, this stable phase develops spontaneous eruptions of non-periodic behavior. Although this behavior itself appears irregular, it can be characterized in a systematic fashion. In particular, parameter-independent features of the spontaneous eruptions may allow useful empirical characterizations of other phenomena that are intrinsically hard to predict and reproduce. Specific features of the distributions of life-times and emergence rates of irregular states display such parameter-independent properties.

© 2004 Elsevier Ltd. All rights reserved.

1. Introduction

Coupled map lattices (CMLs; cf. [6]) are constructed by allowing arrays of dynamically evolving sites to interact through some coupling rule over some defined neighborhood. Time is treated discretely, with an evolution rule determining the state of the system in the next timestep from the state in the current timestep. Space is likewise discrete, as the system consists of a number of discrete cells. The states of individual cells, however, are continuous, and evolve according to some recursive map, typically the standard logistic map. We will use the form of the logistic map

$$f(x) = rx(1 - x), \quad (1)$$

where r is called the logistic parameter. The range of x is taken to be the interval $[0, 1]$, so $f(x)$ remains in this range as long as $r \leq 4$. Discrete time evolution according to $x_{t+1} = f(x_t)$ will display chaotic behavior for most values above the “accumulation point” at $r = 3.56999456\dots$, although “windows” of stable periodic behavior occur in this range as well.

The logistic equation (1) has fixed points, where $f(x) = x$, at $x = 0$ and $x = x' \equiv (r - 1)/r$. The fixed point at $x = 0$ becomes unstable for $r > 2$. For $r > 3$, the fixed point at $x = x'$ is also unstable: this is the start of the period-doubling cascade that eventually leads to chaotic behavior. However, even in the chaotic region, the unstable fixed point plays an important role in the system dynamics. Even in regions where periodicity has been completely lost, all points with

* Corresponding author. Fax: +49 761 207 2199.

E-mail address: haa@igpp.de (H. Atmanspacher).

$x > x'$ map, in the next timestep, to points $x < x'$; and any point in the interval $(1/r) < x < (r-1)/r$ maps onto a point $x > x'$ in the next timestep. Thus, even in a completely chaotic regime, the behavior often shows regular alternations of the sign of $x - x'$. The unstable fixed point x' for a single logistic map continues to play an important role in the behavior of coupled map lattices.

A coupled map lattice is constructed from a group of sites, each individually evolving according to Eq. (1), by defining a neighborhood of sites that interact with the i th site, and a coupling constant ϵ giving the strength of the interaction. A typical evolution equation then becomes

$$x_{i,t+1} = (1 - \epsilon)f(x_{i,t}) + \frac{\epsilon}{N} \sum_{k=1}^N f(x_{k,t}), \quad (2)$$

where the index k is taken to range over the N elements in the neighborhood of the i th cell. In Eq. (2), the timestep considered for the i th cell is the same as for the coupled neighborhood states, thus mimicking an interaction time negligible with respect to the time interval between two successive steps. This is sometimes called “future coupling” [7]. An alternative often used is “causal coupling” where the neighborhood states are taken one timestep earlier, so that the evolution equation becomes

$$x_{i,t+1} = (1 - \epsilon)f(x_{i,t}) + \frac{\epsilon}{N} \sum_{k=1}^N x_{k,t}. \quad (3)$$

Another degree of freedom in the design of a CML is whether the updating of cells is synchronous (all new cell values calculated from the values of the previous timestep are updated simultaneously) or asynchronous (cells are updated one at a time, with the updated cell value used in the calculation of later-updating cells in its neighborhood). (For more details see [7] and [2].) The CMLs examined in the current work all employ future coupling (Eq. 2) and synchronous updating.

A considerable amount of work has been done with one-dimensional CMLs where i is a simple linear index over the entire list of cells. A lesser, although still substantial, body of work has examined the behavior of two-dimensional (2-D) CMLs, essentially starting with Kaneko [5]. In these cases the neighborhoods and boundary conditions are so arranged as to give the lattice a two-dimensional topology. The specific CMLs studied in this work are all square $m \times m$ arrays with periodic boundary conditions in both dimensions. The neighborhood used is in all cases the von Neumann neighborhood of order 1: that is, the neighbors of lattice site x_{ij} are the four sites $x_{i-1,j}$, $x_{i+1,j}$, $x_{i,j-1}$ and $x_{i,j+1}$.

2. Spontaneous emergence of defects and their Brownian motion

As Kaneko [5] has shown, a 2-D CML for a coupling constant $\epsilon = 0.1$ and a logistic parameter in the vicinity of $r = 3.9$ displays a behavior called “Brownian motion of defects”. Once transients die out, the evolution of such a system leads to a stable quasi-periodic “checkerboard” phase in which the state of any given cell and the states of its neighboring cells are on opposite sides of the unstable fixed point. An example is shown in Fig. 1. With each timestep, the cells with $x > x'$ change to values less than x' , and vice versa.

As can be seen from the shading in Fig. 1, the states take on more than two single values. Fig. 2 shows the distribution of state values in Fig. 1, exhibiting four distinct peaks. Each cell, in fact, undergoes a quasi-periodic length-4 cycle in which it visits each of the four peaks in turn, although generally not returning to exactly the same values as on a previous cycle.

For random initial conditions, small patches of the checkerboard phase become visible within a few timesteps of the evolution of the CML. They then spread and invade the irregular regions until those are confined to relatively narrow linear or curvilinear regions between checkerboard domains. These restricted zones of irregular behavior are called defects, or domain walls (by analogy to defects in crystals). They separate two distinct and incompatible phases. For example, a diagonal path along which all cells have $x < x'$ on one side of a defect will have $x > x'$ in all cells on the other side. Fig. 3 shows almost complete confinement of the initial irregular phase.

Once the irregularity is restricted to a set of defects of the minimal thickness (about 2–3 cells) needed to separate incompatible checkerboard regions, the initially curved and jumbled pattern of defects tends to simplify. Local regions of the irregular defects tend to move slowly and randomly. However, in any region where the defect is curved this “Brownian motion” is biased toward the concave side and away from the convex side. As a result, any defect forming a closed curve shrinks until the checkerboard phase in its interior is eradicated; the remaining small irregular region is then eliminated by the surrounding checkerboard. Fig. 4 shows a late stage in such an evolution, where the only remaining defect in the checkerboard is a steadily decaying loop.

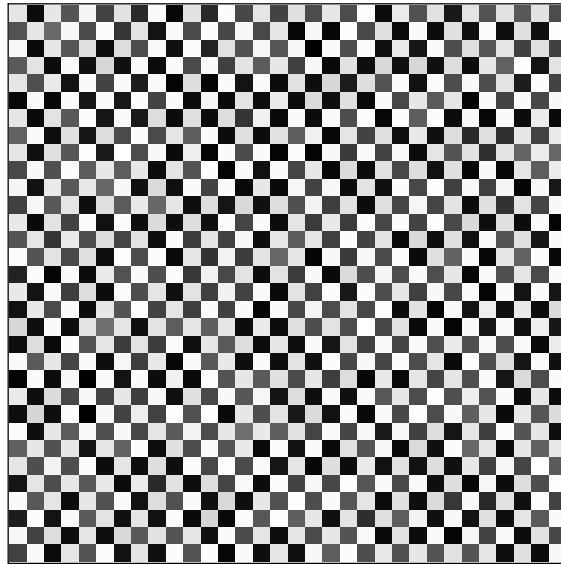


Fig. 1. Illustration of a checkerboard state in a 32×32 CML, $r = 3.9$, $\epsilon = 0.1$. The shades of grey correspond linearly to the cell values; the darker shadings have values below $x' = 0.7436$, the lighter shades have larger values.

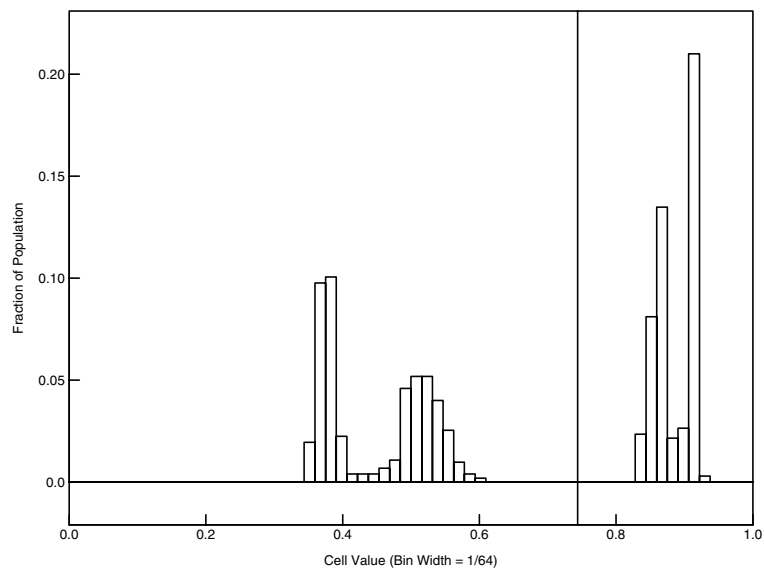


Fig. 2. Histogram of 1024 cell values from Fig. 1. The vertical stroke marks the unstable fixed point $x' = 0.7436$.

While the single-checkerboard state is the stable final state for any CML in this family with even m ,¹ an alternative defect configuration can persist for extremely long times. Fig. 5 shows a situation in which the defects have formed into two lines that cross the entire simulation. Due to the periodic boundary conditions, these lines are actually closed curves, joining themselves across the boundary. The tendency for a defect to move toward its concave side in any locally curved region has the effect of reducing such defects to straight lines. Two such lines in parallel can partition the lattice

¹ If the lattice size m is odd, the lattice space cannot be tiled by a consistent checkerboard and a minimum of one defect, stretching completely across the lattice, is forced.

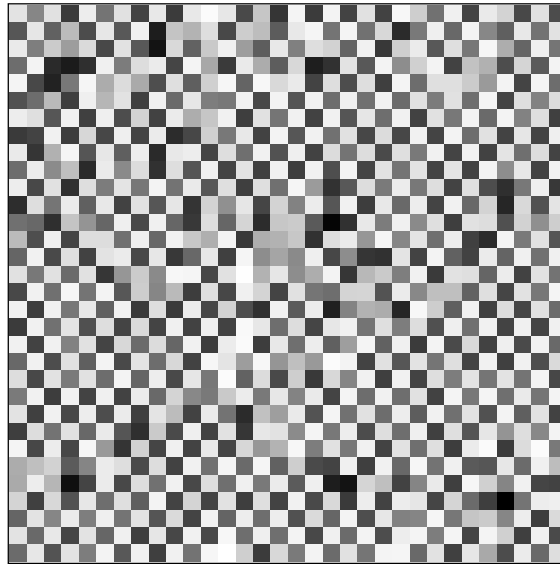


Fig. 3. A 32×32 CML where the initial behavior is confined to domain walls separating incompatible checkerboards. At this early stage the defects remain complicated and tangled.

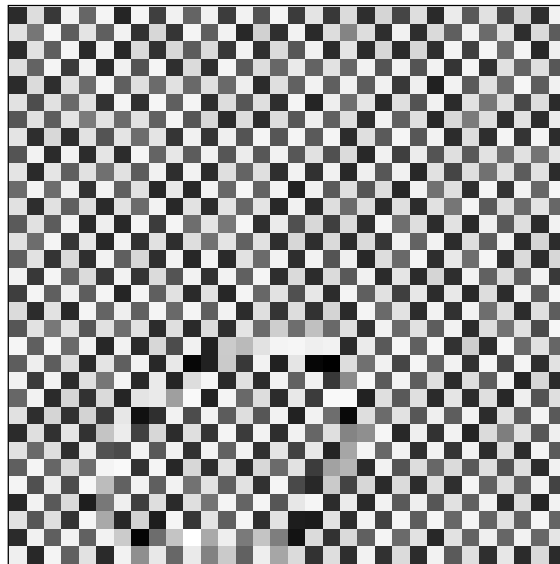


Fig. 4. Late 32×32 CML with decaying loop. The tendency of a curved defect to move toward the direction in which it is concave causes this loop to shrink steadily until it disappears.

into two phases with incompatible checkerboard regions. The only way in which this pattern can then decay is for the random movements of the two defects to bring them into contact. Because the Brownian motion in this case is slow and unbiased, the waiting time for such an event can be extremely long.

If the logistic parameter is increased beyond $r = 3.915$ while $\epsilon = 0.1$, the general behavior described above continues to hold, but the checkerboard phase ceases to be genuinely stable. It becomes subject to spontaneous reversions to irregular behavior. At $r = 3.915$ such reversions are extremely rare, but the frequency of spontaneous outbreaks of irregularity increases with increasing r . Fig. 6 shows this behavior for $r = 3.933$ at a moment when several spontaneous outbreaks are visible.

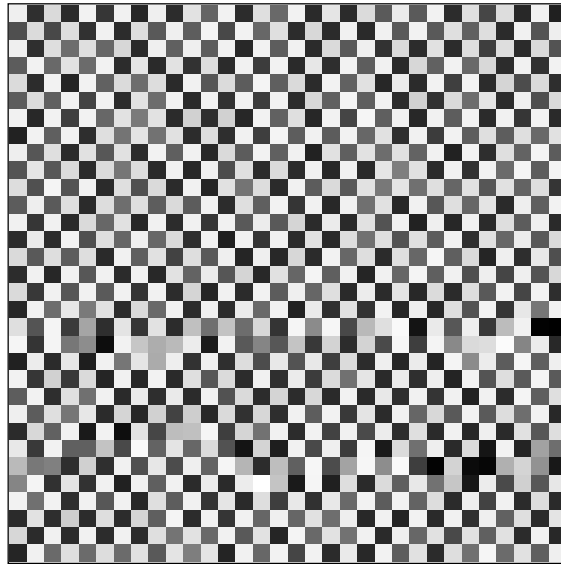


Fig. 5. Metastable configuration with two linear defects across the lattice, meeting themselves at the periodic boundary. The defects cannot decay until their random motions bring them into contact.

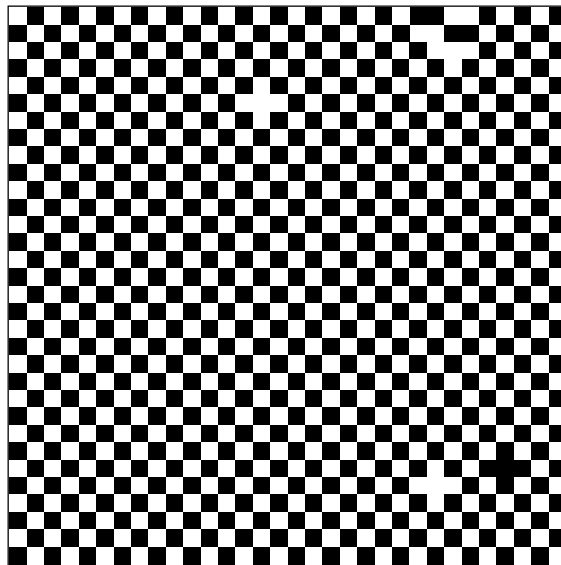


Fig. 6. Spontaneous irregularities in a simulation with $r = 3.933$. To increase visibility of the checkerboard pattern and departures from it, all cells with $x < x'$ are black, those with $x > x'$ are white. All defects resulting from initial conditions have died away thousands of timesteps ago: the departures from the checkerboard pattern are only a few timesteps old.

At $r = 3.935$, the emergence rate of spontaneous irregularities is high enough to keep pace with the ability of the checkerboard phase to spread into irregular regions. Thus, the checkerboard phase loses its dominance in the lattice, which rapidly enters a steady state of continuously maintained spatial and temporal chaos. For the purpose of studying reproducible features of episodic irregularity in CMLs, we therefore restrict ourselves to the parameter range $3.915 < r < 3.935$, where the lattice is dominated by the ordered checkerboard phase.

3. Reproducibility of irregular defects

Reproducibility has been at the center of a number of scientific controversies in recent decades. It is frequently cited as a problem in studies of such controversial phenomena as a putative ability of human consciousness to exert direct influence on physical systems [9,4]. More generally, psychology and, to a lesser extent, other social sciences are notorious for problems with reproducibility (which Epstein [3] related to the notion of stability). And with the study of complex systems, where long-time transients and unstable behavior are the rule rather than the exception, reproducibility has become an issue even in physics. The general question of the limits of standard reproducibility approaches and the ways in which they may fail has recently been discussed from a conceptual and theoretical point of view in [1].

The most common interpretation of a phenomenon that is non-reproducible or hard-to-reproduce under controlled conditions is that it is erroneously reported as a result of flawed experimentation. Another frequently suggested explanation is that experimental variables have not been adequately controlled in experiments, either because of the intrinsic difficulty or impossibility of such control (e.g., in psychological experiments, one cannot erase the subject's memory of intervening experiences to exactly retrieve an earlier mental state), or by current ignorance of the very nature of those variables.

The spontaneous emergence of particular kinds of apparently random behavior, addressed in terms of irregular defects in the preceding section, suggests that some phenomena may be even more fundamentally intractable by standard reproducibility approaches. Some phenomena, especially those involving complex systems with many nonlinearly interacting parts, may be subject to spontaneous and unpredictable changes between regular and irregular behavior.

In spite of the spontaneous emergence of irregular behavior and the innate unpredictability of its appearance, we may nevertheless gain some systematic understanding of their occurrence. The CML model outlined above permits us to explore several questions concerning regime changes between regular and irregular behavior, such as:

- How long do irregular defects last?
- Are subsequent defects independent from each other, or are they affected by prior history?
- How is the behavior of defects related to their frequency or likelihood of appearance?

Since many different kinds of behavior can be generated using CML models with different sets of parameters, a systematic understanding of regime changes between regular and irregular behavior can have considerable impact on specific empirical studies. On the other hand, the significance of those parameters for concrete empirical scenarios is usually not easy to establish, so that CMLs are essentially restricted as a tool for abstractly studying paradigmatic “typical behavior” rather than fitting concrete experiments.

Important results in this respect can be expected where the observed features prove to be parameter-independent, or approximately so. It is reasonable to conjecture that a relation or rule that holds throughout the parameter range of spontaneous regime changes may, in fact, express a property of complex interacting systems that is more general than any specific phenomenological behavior exhibited by CMLs.

4. Results

4.1. General

CMLs are routinely started with random initial conditions and their properties are analyzed after transients have died away. As noted in Section 2, transients may last extremely long. However, unless irregular behavior emerges at a rate high enough to be permanently self-sustaining, the last vestiges of the random initial conditions must eventually die away and produce a lattice that is entirely in the ordered state. While there will often be emergent irregular regions before the last vestiges of the initial random behavior are extinct, the condition of an ordered state covering the entire lattice provides an unambiguous starting point for the analysis of spontaneous outbreaks of irregularities. The first timestep in which the entire lattice is in the ordered state will subsequently be denoted as T_0 .

The visual appearance of defects makes it clear that they are characterized by, and can indeed be defined as, departures from the regular checkerboard pattern in which orthogonal neighbors are always on opposite sides of the unstable fixed point. For purposes of automated analysis, this is taken as the definition of an irregular phase. A cell is counted as being in the regular state if the sign of the quantity $x - x'$ in any given cell is opposite to that of all its orthogonal neighbors. It is counted as being in the irregular state if $x - x'$ has the same sign in the cell and at least one of its orthogonal neighbors.

In the current study we are mainly interested in the local statistics of irregular behavior. How likely is an irregular interval to appear, and how long will it probably last, at any given site in the lattice? The general procedure used to measure these statistics is to monitor each cell in the lattice and record its transitions between regular and irregular states. By recording the times of the most recent transitions in a given cell, it is possible to record, for each incident of spontaneous irregularity, the timestep of its onset, its duration, and the duration of the preceding regular state. To ensure that only spontaneous irregular outbreaks are examined, only irregular phases starting at times $t > T_0$ were considered. For similar reasons, the statistics for regular-state lifetimes (that is, for spontaneous emergence rates) are derived solely from those regular predecessor states starting at times $t > T_0$. Finally, any regular or irregular phases at the end of all runs are also ignored.

It is well-established (cf. [8]) that various measures applied to CMLs may display non-ergodic behavior, which makes it problematic to apply the law of large numbers. Such measures are not mutually independent, for example, at different sites of a lattice or times in its evolution. However, because each simulation starts with a different set of random initial conditions, it is reasonable to suppose that results in different runs of a simulation are statistically independent samples drawn from a generalized space of all possible CML histories.

It was checked that ergodicity in this sense holds indeed and results from different runs are independent. If the variance of a quantity is computed across an ensemble of runs, the uncertainty of the ensemble average scales with the number of runs as the law of large numbers predicts. This applies whether the quantities being averaged are single samples or summaries that encompass an entire run. It does *not* apply, however, to cases where raw data comprising a small part of a run are simply pooled across multiple runs. In this case the data are non-ergodic and standard formulas for the observational uncertainty will be quite unreliable. In view of this fact, statistical inferences, error bars, confidence intervals, and so forth are based on run-wise ensemble averages.

4.2. Emergence rates of spontaneous defects

The mean rate with which spontaneous irregularities emerge depends, of course, strongly upon r . Fig. 7 illustrates this for several characteristic values. At $r = 3.92$, the rate of spontaneous emergence is relatively high for a brief period

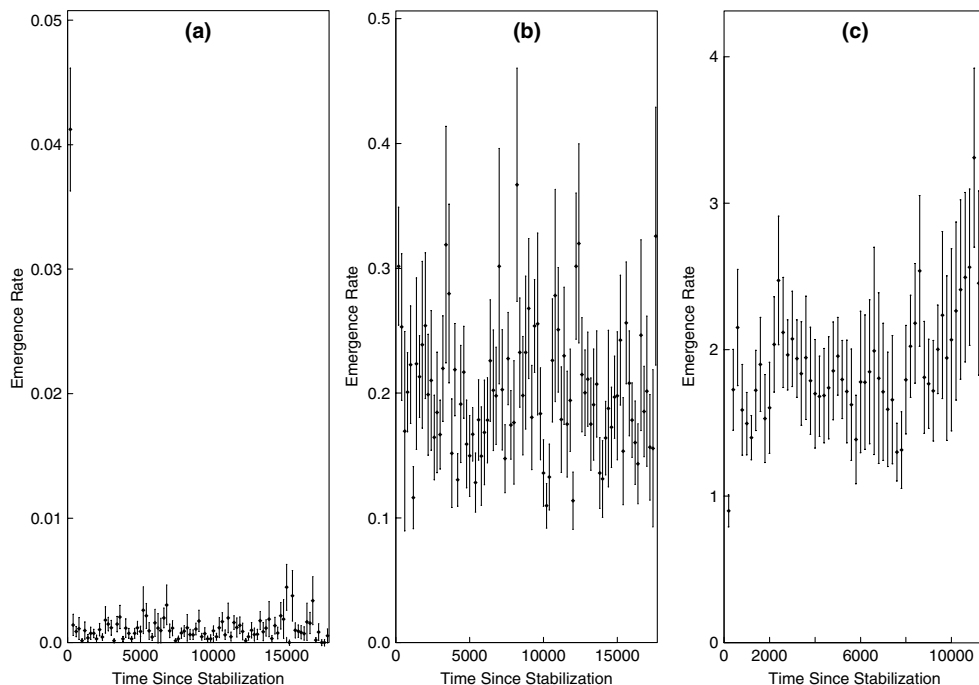


Fig. 7. Spontaneous emergence rates for irregular states as a function of time. Scatter plots show the mean emergence rate of new irregular states per timestep across the full lattice (32×32 ; 1024 cells). Observations are averages over 200 timesteps, plotted as a function of the time after transients: (a) $r = 3.92$. After an initial high value the emergence rate drops to a low value that appears to vary randomly; (b) $r = 3.93$. Emergence rate shows no systematic trend, (c) $r = 3.934$. Emergence rate is suggestive of a slight increase with time.

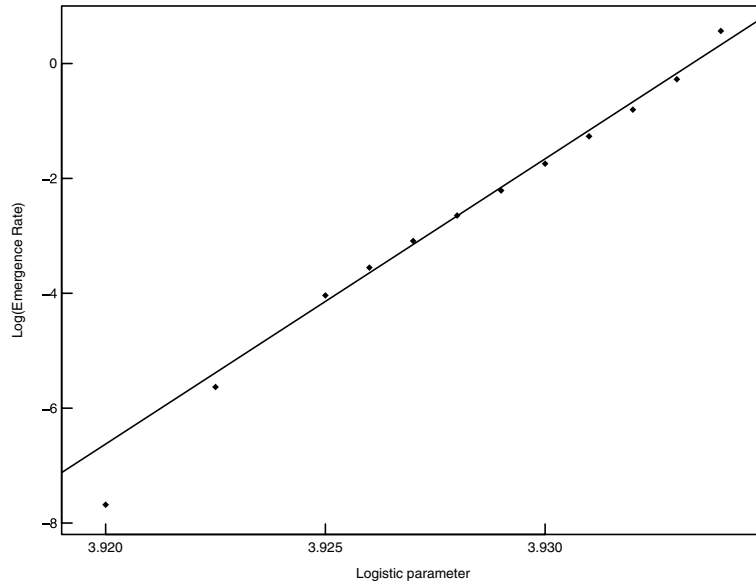


Fig. 8. Mean emergence rate of spontaneous irregularities as a function of r . Log-normal scaling shows exponential behavior as straight lines; the line shown is the best linear regression fit. Error estimates for data points are comparable to icon size.

immediately after the first appearance of a fully ordered state, and then drops to a very low value. The initial high value is most likely a consequence of the temporary enhancement of emergence probabilities for some time after an irregular state has ended; this will be discussed more fully in Section 4.3. Since the end of initial transients is defined by the first appearance of a fully ordered state over the whole lattice, it is guaranteed that there were some actively irregular sites as of the immediately preceding timestep. At $r = 3.92$ the spontaneous emergence rate is so low that this is not generally the case at later epochs. After this initial transient, the low value for the emergence rate shows random excursions but no detectable trend. A linear regression on the data, with the first point excluded, finds a slope indistinguishable from zero.

At $r = 3.93$, the rate of spontaneously emerging irregularities is much higher, and no initial transient is visible; the first point seems comparable to the rest. This is consistent with the explanation of the initial transient for $r = 3.92$; at $r = 3.93$ irregular outbreaks are frequent enough that the typical duration of completely ordered states is relatively short. A linear regression once again detects no trend with time.

Finally, at $r = 3.934$, the rate of outbreaks is still higher and suggests an increasing trend toward higher values. A linear regression finds a positive slope of $(2.93 \pm 1.48) \times 10^{-5}$, which has $p = 0.048$. Since this is the only case showing such a trend, and since the statistical confidence for its existence is marginal, there is no overall evidence for a time-dependent emergence rate. The leftmost point in part (c) of Fig. 7 is somewhat low, and can also be ascribed to a transient effect.

Since any dependence of the overall emergence rate on time, aside from initial transients, is either very small or non-existent, we can average data across the lattice evolution to study the dependence of this mean rate upon r . Fig. 8 illustrates this for the values from Fig. 7 as well as some additional, interpolated values. On the log-normal scale of Fig. 8, the points fall close to a straight line, suggesting approximately exponential dependence of emergence rates on r . The best fit with a slope of 494.6 ± 2.6 is shown. This slope means that increasing the logistic parameter by $\Delta r = 0.0014$ roughly doubles the emergence rate.

Figs. 7 and 8 show that the fairly narrow range $3.92 < r < 3.934$ covers three orders of magnitude in the emergence rate.² Thus, the global rate of spontaneous outbreaks of irregularities is largely time-independent and has a simple dependence on r .

² The range extends from 4.6×10^{-4} to 1.76, in units of outbreaks per timestep per (1024-cell) lattice. As noted in Section 2, occasional spontaneous irregularities can be seen for $r = 3.915$, but their rate is so low that it was impractical to accumulate reliable statistics.

4.3. Lifetimes of regular states

The data tracked for irregular states at particular cells include the duration of the preceding regular state, i.e., how long the cell was in the ordered condition before it went irregular. This allows us to directly, rather than inferentially, test for changes in the emergence rate, which is closely related to the inverse lifetime. If the emergence rate of irregularities (per cell, per timestep) were a uniform constant α , the distribution of lifetimes for regular states should decay exponentially, $L(t) = e^{-\alpha t}$, and the mean lifetime should be $\lambda = \langle L \rangle = 1/\alpha$ (see Appendix A for details).

Because we are primarily interested in the system's behavior after initial transients, the regular-state lifetimes considered in this section are exclusively those intervening between episodes of spontaneous irregularities. Fig. 9 displays that the distribution of those lifetimes does indeed show exponential decay, indicating a constant emergence probability. The distribution for $r = 3.934$ is used as an example because, with its high emergence rate, it provides the most data per run and thus the clearest statistics.

The leftmost point of Fig. 9 shows a strong, non-statistical departure from the linear trend of the rest of the graph. Figs. 10 and 11 focus on the short-lifespan part of this dataset, and display that a well-defined regime change takes place at around a lifetime of 200 timesteps. Longer lifespans decline exponentially, indicating that a regular state which survives at least this long has a constant probability thereafter of decaying into an irregular state. The distribution of shorter lifespans is closely approximated by a power law (Fig. 11). This means that the probability of irregular incidents declines approximately as $1/t$ in this range (see Appendix A).

The changeover from an emergence probability decaying as $1/t$ to a constant probability takes place roughly 150–200 timesteps from the end of the previous irregular state. Fig. 12 shows the empirically estimated time interval within which changeover occurs as a function of r .

4.4. Lifetimes of irregular states

Aside from the probability of emergence of an irregular state, its likely duration is also a question of interest. As proposed in Section 4.3, this duration may be affected by the nature of the precursor, that is, by whether the previous irregular state was part of the initial transient or was itself a spontaneous outbreak. This hypothesis can be investigated empirically by sorting episodes of spontaneous irregularity into two categories: $s \rightarrow s$ states at which a previous irregularity occurred on the same site, and $p \rightarrow s$ states at which the last irregular episode before the current outbreak occurred during the early transient epoch.

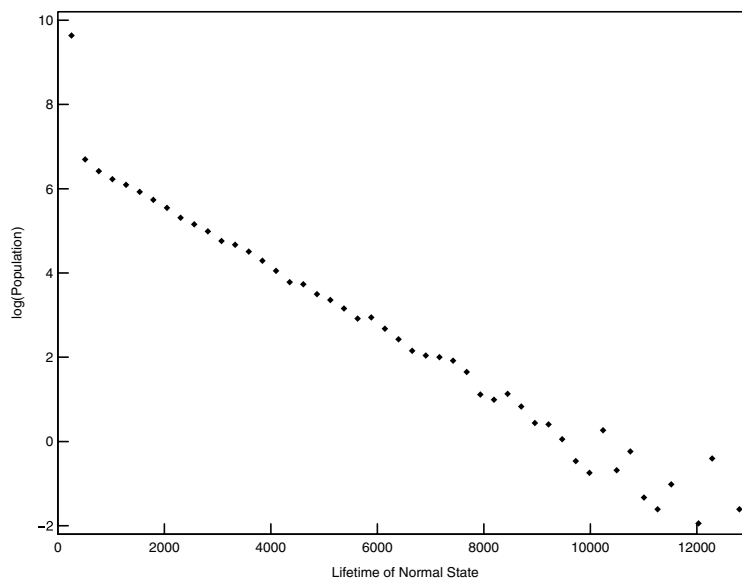


Fig. 9. Exponential decay of the distribution of the lifetimes of regular states for $r = 3.934$. Points are plotted every 256 timesteps and show a run-averaged count of regular states surviving for the indicated length of time. Points at far right are scattered and irregular due to sparse sampling leading to low statistical resolution; in contrast, the single outlier at far left has very good resolution and shows that the exponential relationship breaks down for short lifetimes.

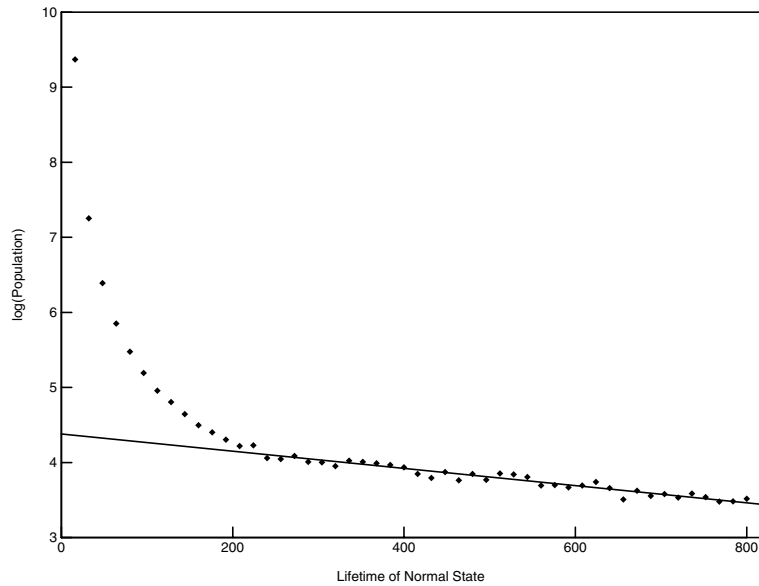


Fig. 10. Different regimes of the distribution of lifetimes of regular states (expanded view of same data as Fig. 9). Points are plotted every 16 timesteps. The right part of the graph is still in the exponential regime: a linear log-normal fit has been plotted to emphasize the contrast to the departure from linearity at left. Changeover to non-exponential decay occurs around 200 timesteps.

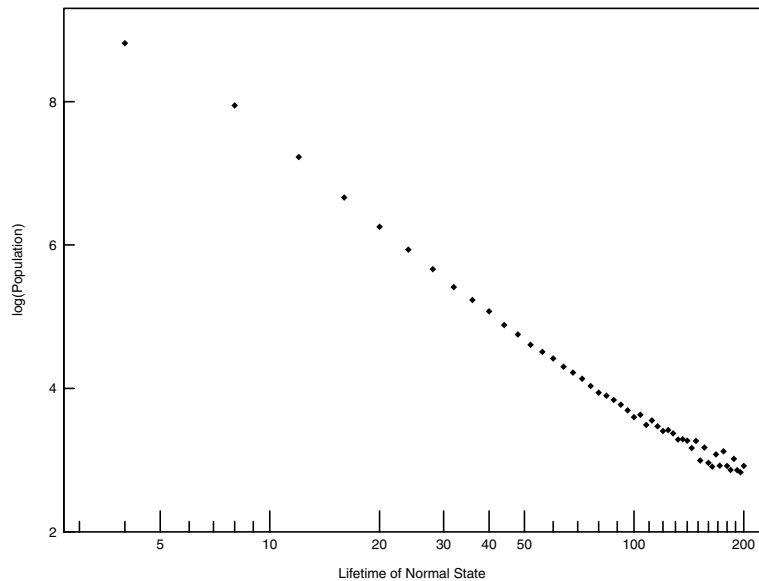


Fig. 11. Approximate power-law decay for short lifetimes of regular states. Data are as in Figs. 9 and 10, but plotted every four timesteps and with x -axis logarithmic. The log-log plot shows behavior close to a power law from timestep 10 onward.

Fig. 13 illustrates that there is an appreciable difference between states with different histories as indicated. Except for lowest values of r , the lifetimes of states with spontaneous predecessors are consistently longer than those of states without them. Underlying causes for this difference are explored in Fig. 14. The data used here are for $r = 3.934$, where the effect is strongest. Rather than pooling all data for a run, Fig. 14 breaks down the data according to two temporal variables: the elapsed time since T_0 , and the duration of regular behavior for each. Comparing Fig. 14 (a) and (b) shows that the lifetimes of states with both kinds of histories decline during the course of the evolution. States with spontaneous predecessors live longer at all stages.

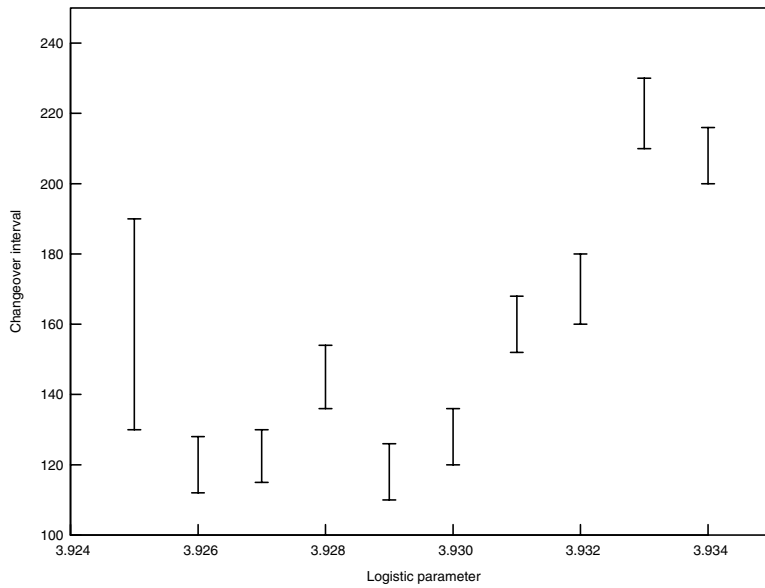


Fig. 12. Changeover intervals between power-law decay to exponential decay as a function of r . Intervals specify the extent of ambiguously curved regions between the two decay regimes. The dependence on r is nonmonotonic with a weakly increasing trend toward higher values of r .

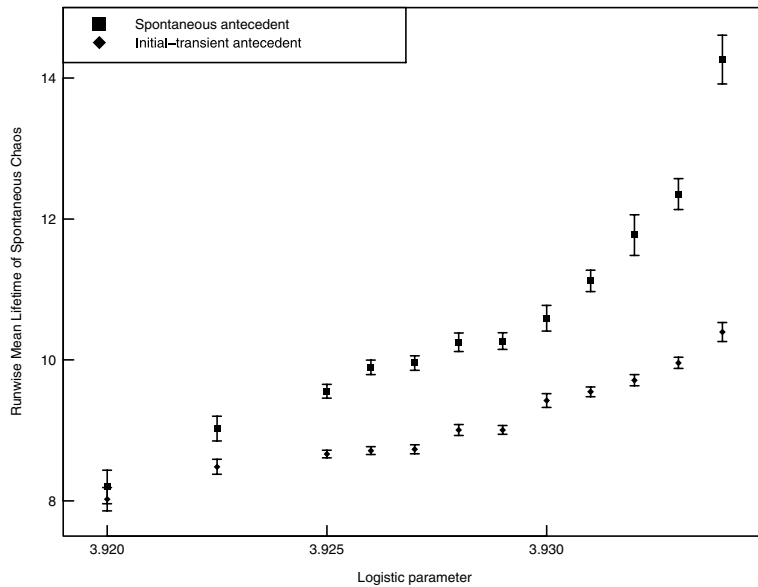


Fig. 13. Mean lifetime of irregular states as a function of r . Error bars refer to the statistical uncertainty of the mean evaluated across multiple simulation runs, not to the width of the lifetime distribution. Diamonds show statistics for states where a previous spontaneous irregularity occurred on the same site; squares show lifetimes for the first spontaneous irregularity since the end of initial transients.

Fig. 14 (c) and (d) suggest that this difference is driven by a dependence on the lifetime of the preceding regular state. In particular, Fig. 14 (c) shows that irregular states emerging after short periods of regular behavior have much longer lifetimes than those emerging after regular behavior has been long established. A more detailed examination (not shown) establishes that this period of extended irregular lifespans occurs during the period of increased irregularity-emergence probability discussed in Section 4.3. Comparing Fig. 14 (c) and (d) shows that spontaneous irregular states

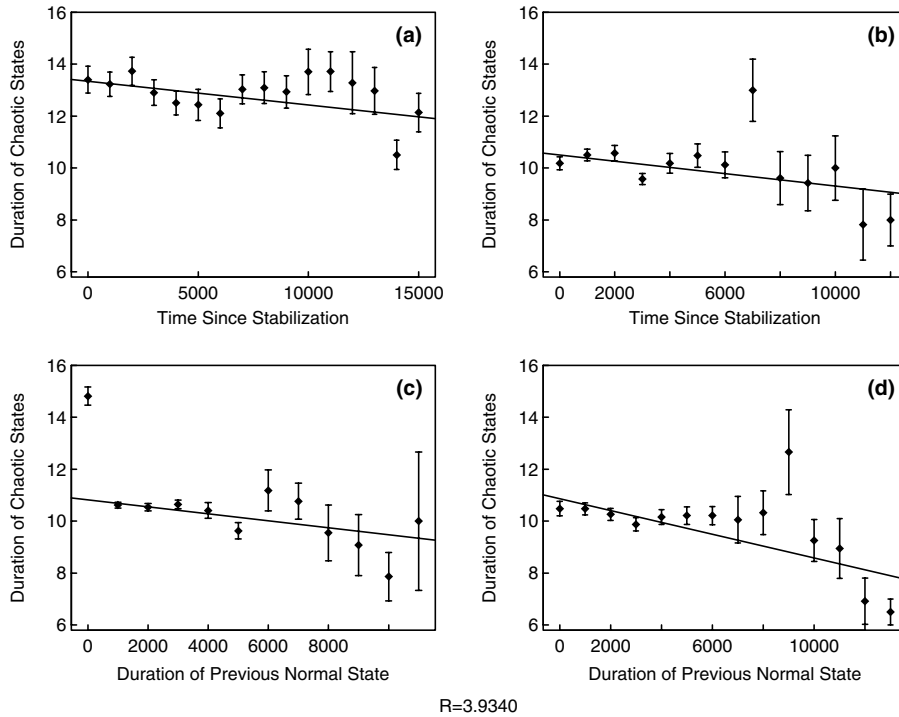


Fig. 14. Influence of temporal variables on the lifetime of irregular states: (a) and (c) plot states where a previous spontaneous irregularity has occurred on the same site; (b) and (d) plot lifetimes of the first irregularity on a site after initial transients. (a) and (b) use, as the x -axis, the time since T_0 , while (c) and (d) use the lifetime of the regular state preceding the irregular state. The plotted lines are least-squares regression fits to all points except the leftmost. Note that there is a pronounced transient in (c) only.

emerging after long interludes of regular behavior follow much the same distribution, no matter whether or not their last irregular antecedents were spontaneous or part of the initial transient. Aside from the first point in Fig. 14 (c), the ongoing decline in Fig. 14 (c) and (d) suggests that the temporal drift in Fig. 14 (a) and (b) is a consequence of a sensitivity to the length of the previous period of regularity; for an increasing evolution time, it becomes possible for longer intervening periods of regularity between irregular outbreaks to occur.

The error bars in Figs. 13 and 14 are based on the statistical variation in mean lifetimes from run to run, not on the actual width of the lifetime distribution. This distribution is shown, for $r = 3.934$, in Fig. 15. Two populations are plotted, for irregularities emerging after short and long periods of regularity. The changeover from “short” to “long” is at 200 timesteps. Aside from the differences in detail, and in their overall statistics, both distributions are substantially similar to each other. The following points apply to the full range of r considered in this work.

- Both distributions are sharply peaked at low values and show extended tails.
- Very short lifespans are strongly suppressed, with almost no irregular states lasting less than 5 timesteps.
- From about 8 to 30 timesteps there is a clear oscillatory behavior in which decay after an even number of timesteps is strongly suppressed. This is presumably due to the natural rhythm of the stable state, discussed in Section 2.
- The distribution for longer lifetimes declines approximately according to a power law with $L(t) \propto t^{-2}$, for odd $t \geq 7$.

Returning to Fig. 13 we may note that over the full range of r the mean duration of irregular states changes by less than a factor of 2, while their rate of emergence changes by a factor of nearly 4000 (Section 4.2). The past history of the emergence site (namely, how long ago it was in an irregular state) exerts an influence comparable in magnitude to the r -dependence. Thus, the characteristic lifetime of irregular states is almost parameter-independent.

The long tails seen in Fig. 15 suggest that the medians of the distributions are considerably lower than their means, which is illustrated in Fig. 16. It is also clear that the median of the lifetime distribution is more stable: its dependence on r is limited to a very narrow range, and it is non-monotonic. Thus, the distribution of lifetimes for spontaneous irregular states has not only a characteristic parameter-independent shape, but also a characteristic, approximately parameter-independent median.

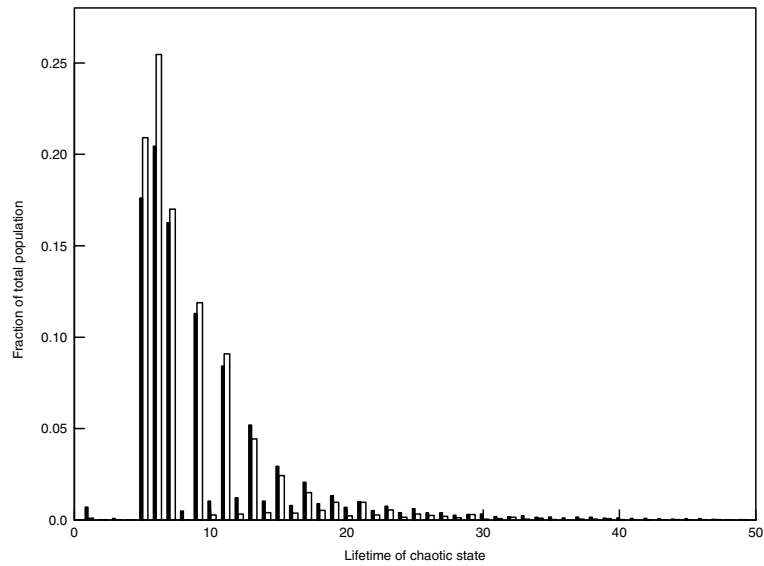


Fig. 15. Distribution of irregular-state lifetimes at $r = 3.934$. Only states with spontaneous irregularities as predecessors are considered. The solid bars to the left of each pair are the population of states emerging after short (<200 timesteps) periods of regular behavior; this population has $\mu = 15.98$, $\sigma = 18.46$. The open bars on the right of each pair are the population of states emerging after long periods of regular behavior: $\mu = 10.51$, $\sigma = 9.91$. Both distributions have long tails extending to the right of the region shown.

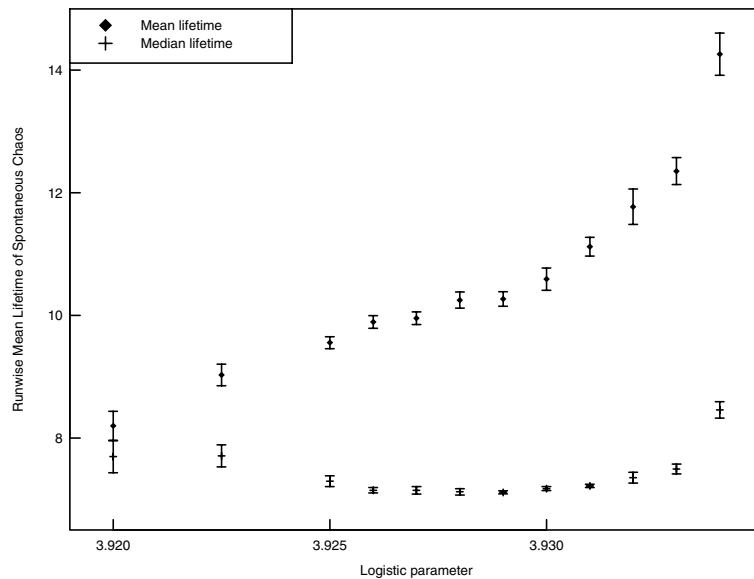


Fig. 16. Mean and median of the distribution of lifetimes of irregular states. The median is a more stable measure, with very weak and non-monotonic dependence on r (cf. Fig. 13).

5. Summary and discussion

The results presented in the preceding section show that spontaneous changes between regular and irregular behavior of coupled map lattices can be characterized in a systematic fashion. For logistic parameters in the range $3.92 < r < 3.934$, the ordered, regular state remains the dominant condition of most of the lattice for most of its history even at the highest rate of spontaneous irregular outbreaks. For $r > 3.934$, the outbreak rate becomes so high

that the simulation displays permanent, ongoing spatiotemporal chaos. In this condition, no further regime changes occur.

Regarding the outbreaks of irregular behavior under predominantly regular conditions, two key questions have been answered:

How long do irregular episodes last?

Within the considered range of parameters, episodes of irregular behavior have a well-defined characteristic lifetime distribution. It is strongly peaked at relatively short values, with a characteristic minimum lifetime, an extensive tail of longer observable lifetimes, and with a median at approximately 125% of the most probable value.

How are irregular episodes affected by local circumstances?

Spontaneous regime changes are most likely to occur at a place and time where and when an outbreak of irregular activity has recently ended. The probability of a renewed regime change is enhanced above its basic background level, decaying as $1/t$, for a period roughly twenty times as long as the median lifespan of the irregular episodes themselves. Moreover, states that appear during this period of enhanced likelihood tend to last longer than others.

Since these features are independent of particular parameters of the coupled map lattice, they permit some definite, if qualitative, predictions for the behavior of a possible class of irregular, difficult-to-reproduce phenomena. As regards the issue of reproducibility in general, intermittent failures to reproduce expected results may be due, in some cases, to inherent spontaneous regime changes in the behavior of the phenomenon under inquiry. This may be tested empirically by evaluating corresponding reports, especially multiple reports with conflicting outcomes, for the qualitative distribution features described above. Such a literature review for selected classes of phenomena is beyond the scope of the current analysis, but offers a promising venue for further work.

Appendix A. Lifetime distributions and decay probabilities

The raw data emerging from a CML tracking the lifetimes of types of states are in the form of a distribution of lifetimes. It is often desirable to convert this distribution into a probability function describing the probability that a state will end (change state) after it has survived a given amount of time.

Although the data are discrete, it is more convenient to consider continuous variables and convert integrals to sum formulas as needed. Therefore, let $L(t)$ be a lifetime density: the fraction of states that survive for a time between t and $t + dt$. By definition

$$\int_{t_0}^{\infty} L(t) dt = 1, \tag{4}$$

where t_0 is a minimum-lifetime origin that will usually be chosen as either 1 or 0 to facilitate computations. The quantity of interest is the transition, or decay, probability $D(t)$, which is the fraction of those states extant at t which will decay between t and $t + dt$. $D(t)$ is by its nature a contingent probability.

Since $L(t)$ is defined as the fraction of states having lifetimes between t and $t + dt$, it may be seen as the fraction of the total initial number of states that will decay *during* the interval $(t, t + dt)$. The total fraction of states surviving as of time t is therefore $1 - \int_{t_0}^t L(\tau) d\tau$. It then follows that

$$D(t) = \frac{L(t)}{1 - \int_{t_0}^t L(\tau) d\tau} = \frac{L(t)}{\int_t^{\infty} L(\tau) d\tau}, \tag{5}$$

where the second form follows from applying Eq. (4) to the denominator. It is also worth noting that when the right-most form of Eq. (5) is used, there is no need to normalize L : multiplying L by any constant factor cancels out.

Some special behaviors of $L(t)$ are of particular interest:

Exponential decay

Take $L(t) = e^{-\alpha t}$, taking advantage of the freedom of normalization noted above. Since $\int_t^{\infty} e^{-\alpha\tau} d\tau = (1/\alpha)e^{-\alpha t}$, $D(t) = e^{-\alpha t}/[(1/\alpha)e^{-\alpha t}] = \alpha$. Eq. (5) thus correctly produces the expected result that an exponentially decaying population is the signature of a constant decay probability.

Power-law decay

Let $L(t) = t^{-\alpha}$. Then $\int_t^{\infty} \tau^{-\alpha} d\tau = \tau^{1-\alpha}/(1-\alpha)|_t^{\infty} = t^{1-\alpha}/(\alpha-1)$. Hence $D(t) = (\alpha-1)/t$; $L(t)$ only decays as a power law if $D(t) \propto t^{-1}$, and the actual exponent of L becomes merely a scaling factor for D .

Eq. (5) is readily convertible to a discrete form

$$D(t) = \frac{L(t)}{\sum_{k=t}^{\infty} L(k)}. \quad (6)$$

This is of limited utility for empirical investigations. As a ratio of random variables it amplifies the fluctuations of its inputs, and it suffers moreover from a discreteness correction which becomes severe for large t . To see this, consider a population of discrete entities with uniform decay probability. Since the population can change only by integer amounts, there must be some final timestep t_f on which the last survivor(s) decay. Since $L(t) = 0$ for all subsequent t , Eq. (6) will compute $D(t_f) = 1$ and becomes undefined for all $t > t_f$, despite the ingoing assumption that $D(t)$ is in fact constant. While the computation becomes truly pathological only at t_f , numerical calculations illustrate that the discreteness correction produces significant distortions long before the last timestep is reached. Section 4.3 therefore does not calculate explicit discrete values of $D(t)$ and takes the more conservative approach of inferring its functional form from the scaling behavior of $L(t)$.

References

- [1] Atmanspacher H, Jahn RG. Problems of reproducibility in complex mind-matter systems. *J Scient Explor* 2003;17(2):243–70.
- [2] Atmanspacher H, Scheingraber H. Inherent global stabilization of unstable local behavior in coupled map lattices. *Int J Bifurcat Chaos* [accepted].
- [3] Epstein S. The stability of behavior. II. Implications for psychological research. *Am Psychol* 1980;35:790–806.
- [4] Jahn R, Dunne B, Bradish G, Dobyns Y, Lettieri A, Nelson R, et al. Mind/machine interaction consortium: PortREG replication experiments. *J Scient Explor* 2000;14(4):499–555.
- [5] Kaneko K. Spatiotemporal chaos in one- and two-dimensional coupled map lattices. *Physica D* 1989;37:60–82.
- [6] Kaneko K, editor. *Theory and applications of coupled map lattices*. New York: Wiley; 1993.
- [7] Mehta M, Sinha S. Asynchronous updating of coupled maps leads to synchronization. *CHAOS* 2000;10:350–8.
- [8] Pikovsky AS, Kurths J. Do globally coupled maps really violate the law of large numbers? *Phys Rev Lett* 1994;72:1644–6.
- [9] Radin DI, Nelson RD. Evidence for consciousness-related anomalies in random physical systems. *Found Phys* 1989;19(12): 1499–514.